

# FluxMem: Adaptive Hierarchical Memory for Streaming Video Understanding

Yiweng Xie<sup>1,2,3</sup>, Bo He<sup>4</sup>, Junke Wang<sup>1,3</sup>, Xiangyu Zheng<sup>1,3</sup>, Ziyi Ye<sup>1,3†</sup>, Zuxuan Wu<sup>1,2,3†</sup>

<sup>1</sup>Institute of Trustworthy Embodied AI, Fudan University, <sup>2</sup>Shanghai Innovation Institute  
<sup>3</sup>Shanghai Key Laboratory of Multimodal Embodied AI, <sup>4</sup>University of Maryland, College Park

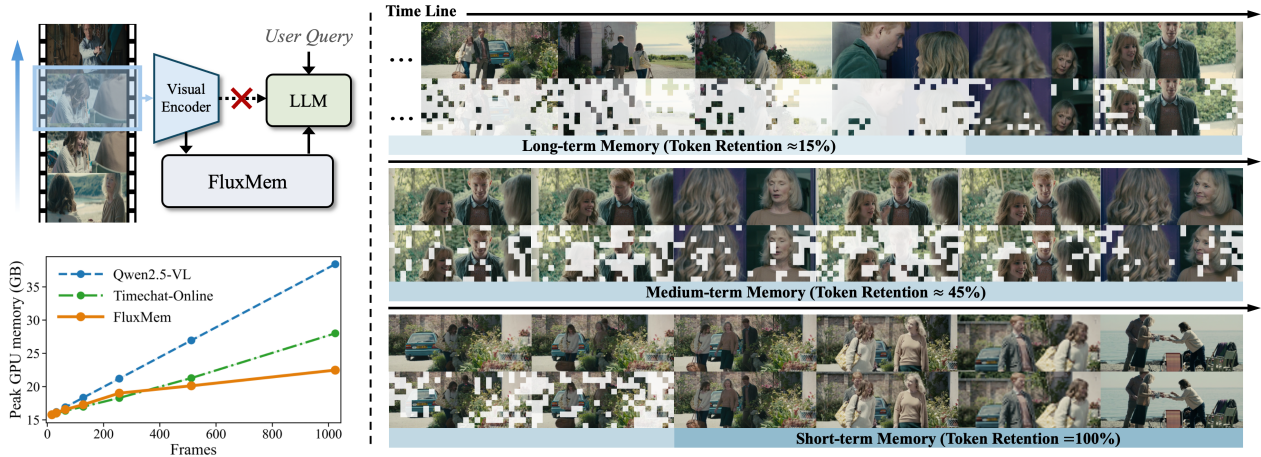


Figure 1. FluxMem is an adaptive hierarchical memory framework to progressively reduce visual tokens for efficient streaming video understanding. **Bottom left:** GPU memory usage vs. video frame length for FluxMem and other methods during inference.

## Abstract

This paper presents **FluxMem**, a training-free framework for efficient streaming video understanding. FluxMem adaptively compresses redundant visual memory through a hierarchical, two-stage design: (1) a Temporal Adjacency Selection (TAS) module removes redundant visual tokens across adjacent frames, and (2) a Spatial Domain Consolidation (SDC) module further merges spatially repetitive regions within each frame into compact representations. To adapt effectively to dynamic scenes, we introduce a self-adaptive token compression mechanism in both TAS and SDC, which automatically determines the compression rate based on intrinsic scene statistics rather than manual tuning. Extensive experiments demonstrate that FluxMem achieves new state-of-the-art results on existing online video benchmarks, reaching 76.4 on StreamingBench and 67.2 on OVO-Bench under real-time settings, while reducing latency by 69.9% and peak GPU memory by 34.5% on OVO-Bench. Furthermore, it maintains strong offline performance, achieving 73.1 on MLVU while using 65% fewer visual tokens. Code is available at <https://github.com/YiwengXie/FluxMem>.

†Corresponding author.

## 1. Introduction

Recently, Multimodal Large Language Models (MLLMs) have achieved significant success in offline video understanding [1, 3, 17, 24, 25, 33, 48, 53]. However, real-world applications such as robotic manipulation [28], autonomous driving [6], and smart glasses [23] demand real-time processing of streaming visual inputs. This poses a critical challenge in effectively memorizing long-term temporal context and producing causal responses to user queries in an online manner [11, 31, 47, 50, 58, 59, 61–63, 65].

To process continuous visual streams in real-time, existing research has primarily focused on three directions: reducing visual tokens prior to the LLM [62, 63], managing the KV cache during the prefill stage [11, 31, 61], and employing text query-guided filtering [7, 37, 62]. Among these, token compression emerges as a more promising approach due to two advantages: (1) unlike KV cache management, it performs deduplication before tokens enter the LLM, offering greater flexibility; (2) unlike query-guided methods, it decouples textual and visual information, enabling the model to dynamically process the visual stream prior to query arrival. However, existing token compression methods such as TimeChat-Online [62] apply a single pruning/merging policy across the stream, overlooking the time-

dependent utility of memory in streaming video. Recent frames require dense preservation for grounding, while distant history tolerates stronger compression. A global policy thus tends to under-prune long-term context and over-prune short-term details critical for causal reasoning.

To address this gap, we introduce **FluxMem**, a training-free framework with an efficient adaptive visual memory design for streaming video understanding. FluxMem segments the visual context into three levels of memory: short-term, mid-term, and long-term, based on their temporal adjacency to the query moment. Accordingly, we propose a progressive visual token reduction strategy based on the hierarchical memory structure: 1) Short-term Memory: all visual information is retained to preserve the immediate perceptual grounding for the current query; 2) Mid-term Memory: Temporal Adjacency Selection (TAS) is applied to reduce temporal redundancy by comparing adjacent frames and removing spatially aligned tokens; 3) Long-term Memory: spatial redundancy within each frame is further reduced by grouping neighboring regions into representative anchors and removing repetitive tokens via Spatial Domain Consolidation (SDC). Unlike previous approaches [4, 42, 58, 62] that rely on manually tuned ratios for token retention or similarity-based thresholds, we derive frame-wise adaptive thresholds based on Otsu’s method [34] for token reduction in the mid- and long-term memory. This adaptive design eliminates manual hyperparameter tuning and ensures robust performance across diverse scene dynamics.

We validate the effectiveness of FluxMem on five video understanding benchmarks across both online and offline tasks. The results demonstrate that FluxMem achieves new state-of-the-art or highly competitive performance across diverse settings. For example, it achieves 53.3 on OVO-Bench [32] and 76.4 on StreamingBench [27] for streaming tasks, and 65.3 on VideoMME [14], 73.1 on MLVU [68], and 61.1 on LongVideoBench [57] for offline evaluation. These results suggest that a single training-free memory framework can consistently improve online and offline video understanding with high efficiency and robustness.

In summary, our main contributions are as follows:

- We introduce a novel training-free hierarchical memory with two lightweight adaptive modules, which equips MLLMs with coherent short- and long-term video modeling for both online and offline settings.
- Our approach achieves state-of-the-art performance on various video tasks in both online and offline settings while discarding 60–70% of visual tokens and reducing latency and GPU memory usage.
- We demonstrate that an adaptive token reduction threshold, based on video-specific information density, outperforms fixed-rule methods. This adaptive capability is natively supported by TAS and SDC.

## 2. Related Work

### 2.1. Multimodal Large Language Models

Recent advances in Multimodal Large Language Models (MLLMs) [25, 51] have broadened their application to video understanding. Typically, these models comprise a visual encoder for extracting frame-level representations, a modality projector to map visual features into the language space, and a Large Language Model (LLM) to generate contextual responses [3, 25, 29, 44, 55, 64, 67]. While these models achieve strong results on standard video benchmarks, they are inherently designed for static, offline settings where the input is the pre-loaded full video rather than a continuous stream. As a result, they fail to adapt to dynamic, real-world scenarios where video frames are processed sequentially and require real-time, temporally coherent, or even proactive responses [20, 27, 32].

### 2.2. Streaming Video Understanding

In contrast to its offline counterpart, streaming video understanding requires models to sequentially process incoming video and generate real-time responses as user queries arrive [20, 27, 32, 35]. In real-world scenarios such as robotic manipulation [28] and autonomous driving [6], models must efficiently manage historical information while focusing on the present context to produce timely and accurate reactions. To address these challenges, recent research has proposed several distinct approaches [11–13, 30, 31, 47, 52, 59, 61, 65]. One line of research concentrates on memory design, which optimizes the storage and retrieval of historical information to alleviate the latency and GPU memory bottlenecks induced by large volumes of visual tokens [31, 61, 65]. A second strategy develops efficient visual token representations, compressing redundant information to improve computational efficiency without compromising semantic fidelity [4, 62]. A third approach introduces additional lightweight MLLMs to enable conventional offline models to proactively respond in streaming settings, effectively transforming them into online models [22, 47].

### 2.3. Visual Token Reduction

Among the numerous visual tokens in MLLM-based video understanding, only a small fraction carries essential semantics, while large portions correspond to repetitive or static regions that contribute little to the overall meaning. This redundancy not only causes significant computational and memory overhead during inference but also complicates cross-modal alignment. To address this issue, visual token reduction is a common solution for the inherent redundancy in videos and the imbalance between the visual and language modalities [10, 16, 38, 40, 49]. Recent studies on visual token reduction can be categorized into three

primary directions. The first focuses on memory compression or temporal redundancy modeling to aggregate long-term information and prevent the accumulation of unnecessary historical tokens [18, 31, 61]. A second strategy is to design adaptive token merging or pruning strategies that dynamically adjust token counts across spatial and temporal dimensions [4, 19, 26, 45, 56, 60]. A third approach introduces language-guided mechanisms that leverage user queries to select the most relevant visual content and efficiently condense visual information [11, 42].

### 3. Method

We propose **FluxMem** (Fig. 2), an Adaptive Hierarchical Memory for spatiotemporal token reduction. FluxMem processes frames on the fly, retaining informative tokens and discarding redundancy in three cooperative parts. (1) a streaming hierarchical memory with short-, mid-, and long-term memory (Sec. 3.1). (2) two lightweight components, Temporal Adjacency Selection (TAS) and Spatial Domain Consolidation (SDC), to guide the dropping and compression of visual tokens (Sec. 3.2). (3) a distribution-adaptive thresholding scheme that derives data-driven thresholds from visual statistics (Sec. 3.3).

#### 3.1. Streaming Hierarchical Memory

The streaming hierarchical memory maintains three cascaded modules to progressively compress while preserving causal consistency [2]. At timestep  $t$ , the streaming video frame  $F_t$  is encoded by a vision encoder into a set of visual tokens  $V_t \in \mathbb{R}^{HW \times D}$ , where each token  $v_{t,h,w} \in \mathbb{R}^D$  corresponds to spatial position  $(h, w)$  within the frame. The memory is composed of  $\mathcal{M}^s, \mathcal{M}^m, \mathcal{M}^l$  with capacity  $c_s, c_m, c_l$ . Visual tokens  $V_t$  are first buffered in short-term memory. Tokens evicted from this level are temporally compressed by TAS (Sec. 3.2) and stored in mid-term memory. If the token count exceeds capacity  $c_m$ , the earliest tokens are evicted to long-term memory, where they are spatially consolidated by SDC (Sec. 3.2). When a user query arrives or a proactive response is triggered (Sec. 3.2), the tokens stored across the memory hierarchy are concatenated while preserving their spatiotemporal structure and then provided to the LLM as visual input for response generation. The streaming procedure is summarized in Algorithm 1.

#### 3.2. Spatiotemporal Token Reduction

To prune visual tokens, FluxMem applies two lightweight, training-free modules: Temporal Adjacency Selection (TAS) at the short-to-mid boundary and Spatial Domain Consolidation (SDC) at the mid-to-long boundary as tokens progress forward through the memory hierarchy. Concretely, we use the cosine distance  $d(x, y) = 1 -$

---

#### Algorithm 1 Streaming procedure of FluxMem

---

**Memory:**  $\mathcal{M}^s, \mathcal{M}^m, \mathcal{M}^l$  with capacities  $c_s, c_m, c_l$   
**modules:** TAS( $\cdot$ ), SDC( $\cdot$ ), ACT( $\cdot$ ); **Threshold:**  $\gamma$

- 1: **while** streaming frame  $F_t$  **do**
- 2:    $V_t \leftarrow \text{Encoder}(F_t)$ ;  $r_t^- \leftarrow \text{ACT}(V_t)$ ;  $\mathcal{M}^s.\text{push}(V_t)$
- 3:   *// response via query or activation trigger*
- 4:   **if** (query  $Q$  arrives) **or** ( $t_a$  exists **and**  $r_t^- > \gamma$ ) **then**
- 5:      $R \leftarrow \text{LLM}(\mathcal{M}^l \oplus \mathcal{M}^m \oplus \mathcal{M}^s, Q)$ ;  $t_a \leftarrow t$
- 6:   *// adaptive hierarchical memory update*
- 7:   **if**  $|\mathcal{M}^s| > c_s$  **then**
- 8:      $O_t^s \leftarrow \mathcal{M}^s.\text{pop}$ ;  $I_t^m \leftarrow \text{TAS}(O_t^s)$ ;  $\mathcal{M}^m.\text{push}(I_t^m)$
- 9:   **if**  $|\mathcal{M}^m| > c_m$  **then**
- 10:      $O_t^m \leftarrow \mathcal{M}^m.\text{pop}$ ;  $I_t^l \leftarrow \text{SDC}(O_t^m)$ ;  $\mathcal{M}^l.\text{push}(I_t^l)$
- 11:   **if**  $|\mathcal{M}^l| > c_l$  **then**
- 12:      $\mathcal{M}^l.\text{evict\_oldest}$
- 13:    $t \leftarrow t + 1$

---

$\cos(x, y)$  and a per-frame, Otsu’s method-derived threshold  $\Theta_t$  (Sec. 3.3) [34] that allows the policy to adapt automatically to scene dynamics. With the arrival of new visual tokens, the hierarchy shifts from motion-centric selection (TAS) to structure-centric consolidation (SDC), turning short-lived dynamics into compact long-range context.

**Temporal Adjacency Selection (TAS).** When the short-term memory overflows at time  $t$ , TAS selectively retains tokens that exhibit significant semantic changes between adjacent temporal frames. Since both neighboring frames are already stored in the short-term buffer when TAS is applied, the causal structure of the token stream is preserved. For each spatial location  $(h, w)$ , we compute the token score as the minimum distance within a  $3 \times 3$  window across adjacent frames:

$$s_{t,h,w}^- = \min_{(i,j) \in \mathcal{N}_{3 \times 3}(h,w)} d(v_{t,h,w}, v_{t-1,i,j}), \quad (1)$$

$$s_{t,h,w}^+ = \min_{(i,j) \in \mathcal{N}_{3 \times 3}(h,w)} d(v_{t,h,w}, v_{t+1,i,j}). \quad (2)$$

Then we compute two separate, data-driven thresholds by applying Otsu’s method (Sec. 3.3) to the distributions of backward-looking scores  $s_{t,h,w}^-$  and forward-looking scores  $s_{t,h,w}^+$  independently, yielding  $\Theta_t^-$  and  $\Theta_t^+$ , respectively.

A token  $(h, w)$  is passed forward as the mid-term memory input if it is considered novel against *either* the past or the future frame, i.e., if  $(s_{t,h,w}^- > \Theta_t^-) \vee (s_{t,h,w}^+ > \Theta_t^+)$ . This union operation ensures that tokens are kept if they represent a significant change from the previous frame *or* a significant change to the next frame. Overall, by detecting redundant tokens via comparing each token to both adjacent frames with a small spatial window, TAS is robust to local misalignment from motion or camera jitter, while highlighting truly changing content without requiring optical flow or

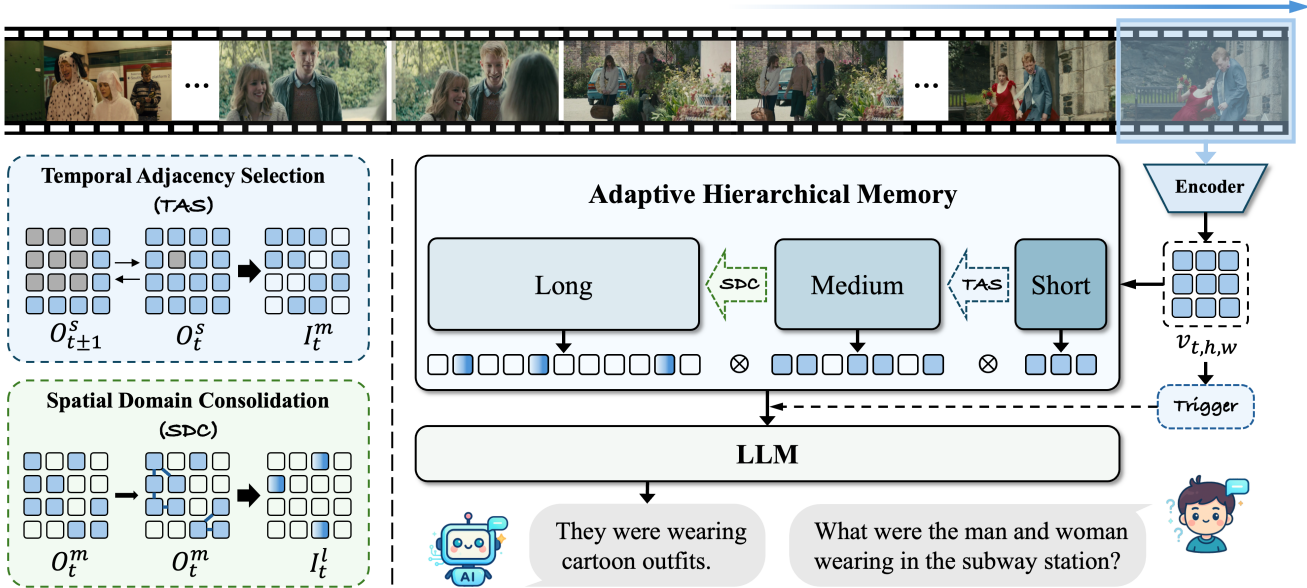


Figure 2. Overview of FluxMem: Adaptive Hierarchical Memory. Each incoming frame is encoded into visual tokens and written to FluxMem in a cascaded short–mid–long process. On short-term memory overflow, Temporal Adjacency Selection (TAS) retains temporally variant tokens for mid-term memory; on mid-term memory overflow, Spatial Domain Consolidation (SDC) merges spatially redundant regions into compact anchors for long-term memory. The overflow process is guided by distribution-adaptive thresholds, autonomously calibrating retention strength to the video’s temporal dynamics. Notably, the similarity metric against the preceding frame, required for TAS, is computed upon the token’s entry into the short-term memory, enabling it to serve as a zero-overhead trigger for active LLM output.

additional heads. The procedure is strictly causal, single-pass, and  $\mathcal{O}(HW)$  per overflow event.

**Spatial Domain Consolidation (SDC).** When the mid-term memory reaches its capacity  $c_m$ , SDC consolidates locally redundant regions from an older frame by operating exclusively on the set of tokens already retained by TAS. For each retained token, we examine other retained tokens that lie within its original  $3 \times 3$  spatial neighborhood and link them if their distance is  $\leq \Theta_t$ , which constructs a sparse, 8-connected graph defined only over this retained set. Here,  $\Theta_t$  is computed from the distribution of these pairwise spatial distances using Otsu’s method (Sec. 3.3). A union-find pass yields connected components  $\{\mathcal{C}_{t,k}\}_k$ . Each component is then replaced by its single mean anchor:

$$a_{t,k} = \frac{1}{|\mathcal{C}_{t,k}|} \sum_{(i,j) \in \mathcal{C}_{t,k}} v_{t,i,j}. \quad (3)$$

$\mathcal{A}_t = \{a_{t,k}\}_k$  is then appended to the long-term memory, with the union-find operator running in near-linear time complexity. Note that this graph is inherently sparse as it is built upon a pre-filtered set of tokens rather than the uncompressed tokens. Replacing each locally coherent region with its barycentric anchor, SDC removes the spatial redundancy while keeping necessary information.

**Proactive Response Triggering.** Online video understanding requires models to develop proactive output ability [47, 54, 62]. We implement this with a zero-cost trigger by reusing TAS statistics to detect scene changes and decide when to respond. Specifically, when frame  $F_t$  enters short-term memory, TAS already computes the backward scores  $s_{t,h,w}^-$  (Eq. (1)). Using these scores, we directly apply Otsu to  $s_{t,h,w}^-$  to obtain  $\Theta_t^-$  and define:

$$r_t^- = \frac{1}{HW} \sum_{h,w} \mathbf{1}[s_{t,h,w}^- > \Theta_t^-]. \quad (4)$$

We declare a scene switch when  $r_t^- > \gamma$ . Here,  $\gamma \in [0, 1]$  is a tunable parameter that controls the trigger sensitivity.

### 3.3. Adaptive Thresholding

Both the TAS and SDC modules rely on a threshold to filter redundant tokens. A fixed, manually-tuned threshold would fail to account for the highly variable dynamics of streaming video, performing poorly in scenes with either very low or high motion. To ensure that our framework is robust and data-driven, we automatically compute all thresholds using Otsu’s method [34]. Otsu’s method is a classic, non-parametric, and efficient algorithm that finds an optimal threshold to partition our similarity scores into two distinct groups for keeping and dropping. It operates by exhaustively searching for the threshold  $\theta$  that maximizes the

Table 1. Results on the real-time subtasks of OVO-Bench and StreamingBench. **OVO-Bench real-time** encompasses: [OCR] Optical Character Recognition; [ACR] Action Recognition; [ATR] Attribute Recognition; [STU] Spatial Understanding; [FPD] Future Prediction; [OJR] Object Recognition. **StreamingBench real-time** encompasses: [OP] Object Perception; [CR] Causal Reasoning; [CS] Clip Summarization; [ATP] Attribute Perception; [EU] Event Understanding; [TR] Text-Rich Understanding; [PR] Prospective Reasoning; [SU] Spatial Understanding; [ACP] Action Perception; [CT] Counting. Best results among open-source models are in **bold** and the best results among training-free methods are underlined. † indicates the reproduced results.

Method	Size	Frames	OVO-Bench real-time							StreamingBench real-time										
			OCR	ACR	ATR	STU	FPD	OJR	Avg.	OP	CR	CS	ATP	EU	TR	PR	SU	ACP	CT	Avg.
<i>Human</i>																				
Human	-	-	94.0	92.6	94.8	92.7	91.1	94.0	93.2	89.5	92.0	93.6	91.5	95.7	92.5	88.0	88.8	89.7	91.3	91.5
<i>Proprietary Models</i>																				
Gemini 1.5 Pro [46]	-	1 fps	85.9	67.0	79.3	58.4	63.4	62.0	69.3	79.0	80.5	83.5	79.7	80.0	84.7	77.8	64.2	72.0	48.7	75.7
GPT-4o [21]	-	64	69.8	64.2	71.6	51.1	70.3	59.8	64.5	77.1	80.5	83.9	76.5	70.2	83.8	66.7	62.2	69.1	49.2	73.3
<i>Open-source Offline MLLMs</i>																				
LongVA [66]	7B	128	-	-	-	-	-	-	-	70.0	63.3	61.2	70.9	62.7	59.5	61.1	53.7	54.7	34.7	60.0
LongVU [39]	7B	1 fps	55.7	49.5	59.5	48.3	68.3	63.0	57.4	-	-	-	-	-	-	-	-	-	-	-
LLaVA-Video [67]	7B	64	69.1	58.7	68.8	49.4	74.3	59.8	63.5	-	-	-	-	-	-	-	-	-	-	-
LLaVA-OneVision [25]	7B	64/32	66.4	57.8	<b>73.3</b>	<b>53.4</b>	71.3	62.0	64.0	80.4	74.2	76.0	80.7	72.7	71.7	67.6	65.5	65.7	45.1	71.1
InternVL2 [9]	8B	64/16	67.1	<b>60.6</b>	63.8	46.1	68.3	56.5	60.4	68.1	60.9	69.4	77.1	67.7	62.9	59.3	53.3	55.0	56.5	63.7
Qwen2.5-VL [3]	7B	64	-	-	-	-	-	-	-	78.3	80.5	79.8	82.4	75.5	80.4	74.1	62.6	67.6	51.1	73.9
<i>Open-source Online MLLMs (Training-Based)</i>																				
VideoLLM-Online [5] [CVPR 2024]	8B	2 fps	8.1	23.9	12.1	14.0	45.5	21.2	20.8	39.1	40.1	34.5	31.1	46.0	32.4	31.5	34.2	42.5	27.9	36.0
Dispider [36] [CVPR 2025]	7B	1 fps	57.7	49.5	62.1	44.9	61.4	51.6	54.6	74.9	75.5	74.1	73.1	74.4	59.9	76.1	62.9	62.2	45.8	67.6
Flash-VStream [65] [ICCV 2025]	7B	1 fps	24.2	29.4	28.5	33.7	25.7	28.8	28.4	25.9	43.6	24.9	23.9	27.3	13.1	18.5	25.2	23.9	48.7	23.2
ViSpeak [15] [ICCV 2025]	7B	1 fps	75.2	58.7	71.6	51.1	74.3	<b>66.9</b>	66.3	79.8	<b>88.3</b>	<b>83.3</b>	81.1	76.4	75.1	70.4	65.9	<b>77.3</b>	34.2	74.4
TimeChat-Online [62] [ACM MM 2025]	7B	1 fps	74.5	48.6	68.1	48.3	69.3	59.8	61.4	80.8	79.7	80.8	83.3	74.8	78.8	78.7	64.2	68.8	<b>58.0</b>	75.3
StreamForest [63] [NeurIPS 2025]	7B	1 fps	68.5	53.2	71.6	47.8	65.4	60.9	61.2	83.1	82.8	82.7	84.3	77.5	78.2	76.9	69.1	75.6	54.4	<b>77.3</b>
<i>Open-source Online MLLMs (Training-Free)</i>																				
ReKV [11] [ICLR 2025]	7B	0.5 fps	-	-	-	-	-	-	-	74.4	78.9	78.6	77.1	68.3	67.9	67.6	62.6	64.3	44.6	69.1
LiveVLM [31] [arXiv 2025]	7B	0.5 fps	-	-	-	-	-	-	-	<b>81.5</b>	78.1	<b>83.3</b>	79.1	69.6	74.1	75.0	<b>69.1</b>	67.7	40.4	72.9
Qwen2.5-VL†	7B	1 fps	79.2	53.2	67.2	51.7	71.3	57.1	63.3	78.3	80.5	79.8	82.4	75.5	80.4	74.1	62.6	67.6	51.1	73.9
<b>FluxMem</b>	7B	1 fps	<b>81.2</b>	<b>59.6</b>	<b>70.7</b>	<b>53.4</b>	<b>75.2</b>	<b>63.0</b>	<b>67.2</b>	80.2	<b>81.1</b>	81.4	<b>85.3</b>	<b>78.0</b>	<b>83.8</b>	<b>80.6</b>	65.9	<b>69.6</b>	<b>52.1</b>	76.4

inter-class variance  $\sigma_B^2(\theta)$ . The optimal, data-driven threshold  $\Theta_t$  at time  $t$  is thus found by:

$$\Theta_t = \arg \max_{\theta} \left[ \omega_1(\theta) \omega_2(\theta) (\mu_1(\theta) - \mu_2(\theta))^2 \right]. \quad (5)$$

where  $\omega_1(\theta)$  and  $\omega_2(\theta)$  represent the class probabilities, and  $\mu_1(\theta)$  and  $\mu_2(\theta)$  are the class means for the two clusters partitioned by the potential threshold  $\theta$ . This process finds the partition that best separates the distribution.

Instead of using a fixed value, we compute the threshold  $\Theta_t$  at runtime based on the target distribution: for TAS, it analyzes the distribution of temporal similarity scores ( $s_{t,h,w}^-$  and  $s_{t,h,w}^+$ ) to adaptively determine the intensity of temporal change; while for SDC, it takes into consideration the distribution of pairwise spatial distances to dynamically assess spatial adjacency relationships. This distribution-adaptive approach allows our reduction policies to automatically adjust their sensitivity to the input data, effectively raising the threshold in high-motion scenes and lowering the threshold in static ones without relying on learnable parameters or manual calibration.

### 3.4. Discussion: Advantages of FluxMem

FluxMem offers four key properties critical for streaming video understanding: (i) training-free operation, (ii) strict online causality, (iii) hierarchical memory organization, and (iv) adaptive compression.

**Training-free vs. Training-based.** Online MLLMs, such as Flash-VStream [65], require task-specific fine-tuning, which increases deployment costs and limits model generality. In contrast, FluxMem addresses this limitation by operating as a training-free, plug-and-play module. It leverages on-the-fly similarity statistics through its TAS and SDC components, ensuring seamless compatibility with any pre-trained MLLM without the need for additional fine-tuning.

**Online-causal vs. Offline-global.** Unlike conventional offline systems that rely on global keyframe selection [43] or retrospective memory construction [40], FluxMem processes data in a strictly causal, hierarchical cascade. This design ensures real-time processing and long-horizon applicability, making FluxMem well-suited for continuous streaming tasks where temporal causality must be maintained throughout.

Table 2. Results on the online video understanding benchmarks **OVO-Bench** and **StreamingBench real-time**, as well as on the offline benchmarks **VideoMME (w/o sub.)**, **MLVU**, and **LongVideoBench**. Here, “w/o sub.” denotes evaluation on VideoMME without subtitles. Best overall results are in **bold** and the best results among training-free methods are underlined. † indicates the reproduced results.

Method	Size	Frames	Online Video		Offline Video					
			StreamingBench	OVO-Bench	VideoMME			MLVU	LongVideoBench	
			Real-Time	Overall	Short	Medium	Long	All	M-Avg	Val
<i>Open-source Offline MLLMs</i>										
LongVA [66]	7B	128	60.0	–	61.1	50.4	46.2	52.6	56.3	–
LongVU [39]	7B	1 fps	–	48.5	–	–	–	60.6	65.4	–
LLaVA-Video [67]	7B	1 fps	–	53.1	–	–	–	63.3	70.8	–
LLaVA-OneVision [25]	7B	32	71.1	52.9	70.1	56.4	48.8	58.4	64.7	56.5
InternVL2.5 [8]	8B	64	–	–	–	–	–	64.2	68.9	60.0
Qwen2.5-VL [3]	7B	768	73.7	–	–	–	–	65.1	70.2	56.0
<i>Open-source Online MLLMs (Training-Based)</i>										
VideoLLM-Online [5] [CVPR 2024]	8B	2 fps	36.0	–	–	–	–	–	–	–
Dispider [36] [CVPR 2025]	7B	1 fps	67.6	41.8	–	53.7	49.7	57.2	61.7	–
VideoChat-Online [20] [CVPR 2025]	4B	2 fps	–	–	–	–	44.9	52.8	–	–
Flash-VStream [65] [ICCV 2025]	7B	1 fps	23.2	33.6	72.0	61.1	50.3	61.2	–	–
TimeChat-Online [62] [ACM MM 2025]	7B	1 fps	75.3	47.6	–	–	52.4	63.3	65.4	57.7
StreamForest [63] [NeurIPS 2025]	7B	1 fps	<b>77.3</b>	<b>55.6</b>	–	–	–	61.9	69.6	–
<i>Open-source Online MLLMs (Training-Free)</i>										
MovieChat [41] [CVPR 2024]	7B	2048	–	–	–	–	33.4	38.2	–	–
ReKV [11] [ICLR 2025]	7B	0.5 fps	69.1	–	–	–	–	–	68.5	–
StreamChat [58] [ICLR 2025]	8B	1 fps	64.7	–	–	–	–	–	–	–
LiveVLM [31] [arXiv 2025]	7B	0.5/0.2 fps	72.9	–	66.7	56.4	48.8	57.3	66.3	–
StreamMem [61] [arXiv 2025]	7B	4.0/0.5 fps	–	–	71.5	62.4	52.3	62.1	65.9	–
Qwen2.5-VL†	7B	1 fps	73.9	49.8	73.8	62.4	53.8	63.3	67.9	60.7
<b>FluxMem</b>	7B	1 fps	<u>76.4 (+2.5)</u>	<u>53.3 (+3.5)</u>	<u>76.9 (+3.1)</u>	<u>65.1 (+2.7)</u>	<u>54.0 (+0.2)</u>	<u>65.3 (+2.0)</u>	<u>73.1 (+5.2)</u>	<u>61.1 (+0.4)</u>

**Hierarchical vs. Monolithic memory.** Most prior memory designs rely on a flat buffer or a single-stage pruning module, which can disrupt temporal coherence or spatial structure. FluxMem adopts a hierarchical, cascaded scheme: TAS preserves temporally novel tokens, while SDC consolidates spatial redundancies at a coarser granularity. This staged organization aligns with the intrinsic spatiotemporal hierarchy of video data, allowing the model to preserve salient long-range dependencies while yielding compact, spatial-preserving representations during streaming.

**Adaptive vs. Fixed Heuristics.** Typical pruning-based methods [4, 62] rely on fixed ratios or manually tuned thresholds, which fail to adapt to dynamic scene variations. In contrast, FluxMem employs per-frame Otsu-based thresholds that automatically adjust the pruning strength, ensuring effective reduction while preserving important information in both static and fast-moving scenes.

## 4. Experiments

### 4.1. Implementation Details

In our experiments, we implement FluxMem based on Qwen2.5-VL-7B [3], since it is the current state-of-the-art video-language model. For online benchmarks, videos are sampled at 1 fps to simulate real-time input, with up to 256 visual tokens per frame and 256 frames per video. We set short-term memory length to 8 frames, mid-term memory length to 64, and assign the remaining frames to long-term memory, which can preserve long-range temporal context.

For offline benchmarks, we also use 1 fps, reducing per-frame tokens to 64 and limiting the maximum sequence length to 1024 frames. We set short-, mid-, and long-term memory lengths as 8, 512, and the rest of the frames, respectively. This provides a balanced trade-off between efficiency and the global temporal coverage. All experiments are conducted on  $8 \times$  A100 GPUs.

### 4.2. Benchmarks

To evaluate the effectiveness of the FluxMem, we conduct experiments on both online and offline video understanding benchmarks. For the online evaluation, we adopt OVO-Bench [32] and StreamingBench [27]. OVO-Bench evaluates timestamp-based understanding of streaming video, covering historical retrieval, real-time awareness, and proactive response. StreamingBench evaluates models on real-time visual, omni-source, and contextual understanding. Our analysis concentrates on the real-time sub-task. For the offline evaluation, we choose VideoMME [14], MLVU [68], and LongVideoBench [57]. VideoMME offers full-spectrum multimodal assessment across diverse domains and durations; MLVU targets long-video multi-task understanding with minutes- to hours-long clips; and LongVideoBench focuses on long-context referring reasoning with extended video-language sequences.

### 4.3. Results on Online Video Understanding

As shown in Table 1, FluxMem achieves strong performance in real-time evaluation. On StreamingBench,

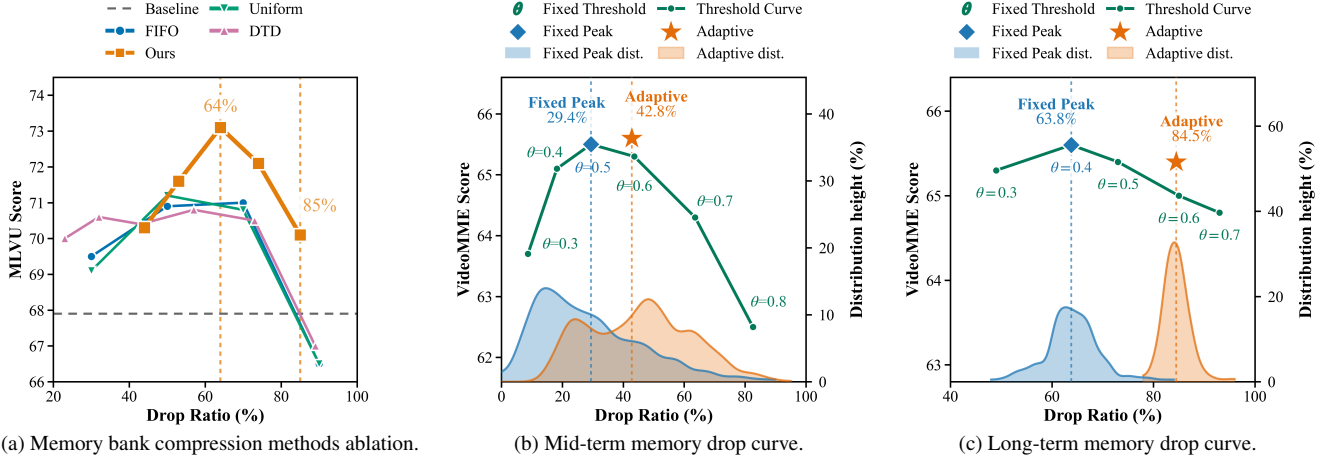


Figure 3. Ablation of FluxMem. (a) Method comparison across drop ratios on the MLVU dataset. (b) and (c) Comparison of our adaptive and fixed thresholds in the mid- and long-term memory banks. The cosine distance of each token is compared against these thresholds to determine whether it is kept or dropped. The shaded area presents the distribution of average per-video drop ratios for the adaptive and optimal fixed thresholds, aggregated across all videos in the MLVU benchmark.

FluxMem improves the Qwen2.5-VL from 73.9 to 76.4 while compressing roughly 70% of visual tokens. On OVO-Bench, FluxMem improves real-time and overall from 63.3 to 67.2 and from 49.8 to 53.3, respectively (Table 2). Notably, significant gains could be observed in tasks that demand both short-horizon cues and stable temporal context, such as Prospective Reasoning (+6.5) and Spatial Understanding (+3.3) on StreamingBench, as well as Action Recognition (+6.4) and Object Recognition (+5.9) on OVO-Bench. We believe these improvements result from the hierarchical memory that preserves recent details while reducing temporal and spatial redundancy through TAS and SDC jointly. Among online MLLMs, FluxMem achieves strong overall performance, surpassing LiveVLM [31] and TimeChat-Online [62]. These results highlight the ability of FluxMem to distill salient information from highly redundant video streams and deliver state-of-the-art online reasoning without task-specific training.

#### 4.4. Results on Offline Video Understanding

As shown in Table 2, FluxMem outperforms the baseline on offline video QA benchmarks, despite being designed for online understanding and using significantly fewer tokens. Specifically, it achieves 65.3 (vs. 63.3) on VideoMME, 73.1 (vs. 67.9) on MLVU, and 61.1 (vs. 60.7) on LongVideoBench. These results surpass all training-free and training-based methods, validating FluxMem as a highly generalizable, training-free framework that demonstrates strong efficacy on offline long-video benchmarks by excelling at salient information distillation. Experiments on VideoMME subtasks validate the efficacy of FluxMem. The model achieves significant gains in both short (from 73.8 to 76.9) and medium (from 62.4 to 65.1) contexts. More crit-

Table 3. Efficiency comparison between the baseline and FluxMem. “↓” indicates reduction vs. baseline.

Dataset	Method	Latency↓ (ms)	Peak Mem↓ (GB)	Perf.↑
MLVU	Baseline	3614	41.3	67.9
	FluxMem	2014 (↓ 44.3%)	28.4 (↓ 31.2%)	73.1
OVO-Bench	Baseline	2701	35.8	49.8
	FluxMem	812 (↓ 69.9%)	23.5 (↓ 34.5%)	53.3

ically, performance in long contexts remains stable (from 53.8 to 54.0) even under an aggressive token reduction regime approaching 90%. These results indicate that the hierarchical design integrating TAS and SDC successfully retains salient tokens while discarding redundancy, thereby enhancing global understanding.

#### 4.5. Ablation Studies

**Efficiency.** Beyond accuracy, FluxMem substantially improves deployment efficiency. To isolate the contribution of the memory mechanism, we pre-extract frame-level visual features and measure the cost after vision encoding in Table 3. On OVO-Bench, FluxMem cuts latency by 69.9% and memory by 34.5% while improving accuracy by +3.5. On MLVU, it reduces latency and memory by 44.3% and 31.2% with +5.2 accuracy. In the online setting, the per-frame update introduces only 4.1 ms overhead in total (1.3 ms for TAS, 2.4 ms for SDC and 0.4 ms for others), preserving real-time efficiency.

**Effect of Hierarchical Memory.** To evaluate the contributions of short-term (S), mid-term (M), and long-term (L) memory components, we conduct ablations by selectively

Table 4. Ablation of the memory module. “↓” denotes average token drop ratio across all benchmarks. Best results are in **bold**.

Memory part				MLVU	VideoMME	StreamingBench	Score
S	M	L	Visual Tokens	M-Avg	w/o sub.	real-time	Avg.
✓	×	×	↓ 0.0%	67.8	63.3	73.9	68.3
×	✓	×	↓ 43.2%	69.9	65.5	74.7	70.0
×	×	✓	↓ 85.1%	70.9	62.0	75.9	69.6
✓	✓	×	↓ 42.4%	70.0	<b>65.6</b>	74.9	70.2
✓	×	✓	↓ 83.6%	70.9	61.9	<b>77.0</b>	69.9
×	✓	✓	↓ 65.6%	<b>73.1</b>	65.4	75.8	71.4
✓	✓	✓	↓ 64.3%	<b>73.1</b>	65.3	76.4	<b>71.6</b>

enabling or removing each module. The results in Table 4 yield three consistent observations: (i) Complementary effects across different levels of memory. On MLVU, combining M and L reaches the highest accuracy of 73.1 while removing 65.6% of visual tokens, outperforming models using only M or L. This indicates that TAS captures temporal variation and SDC captures spatial structure, and their roles become mutually reinforcing. (ii) Necessity of short-term memory for online perception. On real-time streaming tasks in StreamingBench, preserving the short-term memory stabilizes short-horizon perception. The S+L configuration attains an accuracy of 77.0, higher than using only S at 73.9 or only L at 75.9, showing that fine-grained short-range cues remain crucial for online understanding even when long-term memory is aggressively compressed. (iii) Balanced accuracy–efficiency trade-off. The full (S+M+L) hierarchy attains the highest overall accuracy of 71.6 with 64.3% of token reduction, remaining stable across both online and offline tasks. Using only S preserves too much redundancy, while using only L can remove subtle but important cues.

### Comparison of Different Token Reduction Methods.

Figure 3(a) compares our method with different token reduction strategies, including FIFO, Uniform, Random, and DTD [62]. All methods exhibit a similar trend: performance first improves and then gradually declines as the drop ratio increases. Within the practical 50–70% range, FluxMem consistently outperforms all counterparts, including the training-free DTD method used in TimeChat-Online [62]. Notably, FluxMem achieves an accuracy of 73.1 on MLVU at a 64% drop ratio, and still maintains 70.1 even under an aggressive 85% token drop. We believe the superior performance stems from the structured hierarchical memory built upon the TAS and SDC modules.

**Analysis of Adaptive Thresholding.** We compare adaptive and fixed thresholds on MLVU [68] in Figure 3(b) and Figure 3(c). In the mid-term memory, the best fixed threshold achieves 65.5 (◆ in (b)) at a 29.4% drop ratio, whereas the adaptive threshold attains 65.6 (★ in (b)) at

Table 5. Ablation study of FluxMem and SFT on the Qwen2.5-VL. Performance is evaluated on OVO-Bench (Overall) and StreamingBench (real-time). The SFT was performed on a subset of data from TimeChat-Online-139K [62] and VideoChatOnline-IT [20].

Method	OVO-Bench	StreamingBench
Qwen2.5-VL	49.8	73.9
+ FluxMem	53.3 (+3.5)	76.4 (+2.5)
+ FluxMem + SFT	61.4 (+11.6)	76.7 (+2.8)

a substantially higher 42.8% drop ratio, indicating more efficient compression without sacrificing accuracy. In the long-term memory, the best fixed threshold reaches 65.6 (◆ in (c)) at 63.8% compression, while the adaptive threshold obtains a comparable 65.4 (★ in (c)) at a much higher 84.5% drop ratio. Beyond this accuracy–compression trade-off, the threshold distributions further reveal distinct behaviors across memory levels: in the mid-term memory, adaptive thresholds form a clear multi-peak distribution that reflects diverse inter-frame dynamics, whereas fixed thresholds collapse into a diffuse single mode; in the long-term memory, adaptive thresholds concentrate into a sharp single peak, suggesting a stable operating point induced by the more regular spatial redundancy and further reinforced by SDC, while fixed thresholds remain scattered. Overall, these results show that adaptive thresholding flexibly captures temporal variability in mid-term memory while maintaining stable spatial reduction in long-term memory, consistently delivering stronger hierarchical token compression without manual tuning.

**Training-free vs. SFT.** As shown in Table 5, FluxMem not only improves the Qwen2.5-VL baseline under the training-free setting, but also remains competitive with supervised fine-tuning. Specifically, after applying SFT on a small subset of online video datasets [20, 62], the performance of our model is significantly improved on both OVO-Bench overall and StreamingBench real-time.

## 5. Conclusion

This paper introduces FluxMem, a training-free, plug-and-play framework that enables large multimodal models to effectively and efficiently process long streaming video sequences. FluxMem maintains a hierarchical memory with two key components: Temporal Adjacency Selection and Spatial Domain Consolidation, which mitigate spatiotemporal redundancy while respecting causality. Experiments across both online and offline benchmarks have demonstrated that FluxMem consistently outperforms all existing training-free methods, and even surpasses training-based methods. We believe FluxMem offers valuable insights for future research on streaming video understanding.

## Acknowledgments

This work was supported by the National Natural Science Foundation of China (No.62472098) and the Science and Technology Commission of Shanghai Municipality (No.24511103100).

## References

- [1] Anthropic. Claude Sonnet 4.5. <https://www.anthropic.com/news/claude-sonnet-4-5>, 2025. 1
- [2] Richard C. Atkinson and Richard M. Shiffrin. Human memory: A proposed system and its control processes. In *The Psychology of Learning and Motivation*, pages 89–195. Academic Press, 1968. 3
- [3] Shuai Bai, Keqin Chen, Xuejing Liu, Jialin Wang, Wenbin Ge, Sibao Song, Kai Dang, Peng Wang, Shijie Wang, Jun Tang, Humen Zhong, Yuanzhi Zhu, Mingkun Yang, Zhaohai Li, Jianqiang Wan, Pengfei Wang, Wei Ding, Zheren Fu, Yiheng Xu, Jiabo Ye, Xi Zhang, Tianbao Xie, Zesen Cheng, Hang Zhang, Zhibo Yang, Haiyang Xu, and Junyang Lin. Qwen2.5-vl technical report. *arXiv preprint arXiv:2502.13923*, 2025. 1, 2, 5, 6
- [4] Daniel Bolya, Cheng-Yang Fu, Xiaoliang Dai, Peizhao Zhang, Christoph Feichtenhofer, and Judy Hoffman. Token merging: Your ViT but faster. In *ICLR*, 2023. 2, 3, 6
- [5] Joya Chen, Zhaoyang Lv, Shiwei Wu, Kevin Qinghong Lin, Chenan Song, Difei Gao, Jia-Wei Liu, Ziteng Gao, Dongxing Mao, and Mike Zheng Shou. Videollm-online: Online video large language model for streaming video. In *CVPR*, 2024. 5, 6
- [6] Li Chen, Penghao Wu, Kashyap Chitta, Bernhard Jaeger, Andreas Geiger, and Hongyang Li. End-to-end autonomous driving: Challenges and frontiers. *IEEE Transactions on Pattern Analysis and Machine Intelligence*, 2024. 1, 2
- [7] Liang Chen, Haozhe Zhao, Tianyu Liu, Shuai Bai, Junyang Lin, Chang Zhou, and Baobao Chang. An image is worth 1/2 tokens after layer 2: Plug-and-play inference acceleration for large vision-language models. In *ECCV*, pages 19–35. Springer, 2024. 1
- [8] Zhe Chen, Weiyun Wang, Yue Cao, Yangzhou Liu, Zhangwei Gao, Erfei Cui, Jinguo Zhu, Shenglong Ye, Hao Tian, Zhaoyang Liu, et al. Expanding performance boundaries of open-source multimodal models with model, data, and test-time scaling. *arXiv preprint arXiv:2412.05271*, 2024. 6
- [9] Zhe Chen, Weiyun Wang, Hao Tian, Shenglong Ye, Zhangwei Gao, Erfei Cui, Wenwen Tong, Kongzhi Hu, Jiapeng Luo, Zheng Ma, et al. How far are we to gpt-4v? closing the gap to commercial multimodal models with open-source suites. *Science China Information Sciences*, 67(12):220101, 2024. 5
- [10] Chuanqi Cheng, Jian Guan, Wei Wu, and Rui Yan. Scaling video-language models to 10k frames via hierarchical differential distillation. *ICML*, 2025. 2
- [11] Shangzhe Di, Zhelun Yu, Guanghao Zhang, Haoyuan Li, Hao Cheng, Bolin Li, Wanggui He, Fangxun Shu, Hao Jiang, et al. Streaming video question-answering with in-context video kv-cache retrieval. In *ICLR*, 2025. 1, 2, 3, 5, 6
- [12] Xin Ding, Hao Wu, Yifan Yang, Shiqi Jiang, Donglin Bai, Zhibo Chen, and Ting Cao. Streammind: Unlocking full frame rate streaming video dialogue through event-gated cognition. *ICCV*, 2025.
- [13] Saul José Rodrigues dos Santos, António Farinhas, Daniel C McNamee, and André FT Martins.  $\infty$ -video: A training-free approach to long video understanding via continuous-time memory consolidation. *ICML*, 2025. 2
- [14] Chaoyou Fu, Yuhan Dai, Yongdong Luo, Lei Li, Shuhuai Ren, Renrui Zhang, Zihan Wang, Chenyu Zhou, Yunhang Shen, Mengdan Zhang, et al. Video-mme: The first-ever comprehensive evaluation benchmark of multi-modal llms in video analysis. In *CVPR*, 2025. 2, 6
- [15] Shenghao Fu, Qize Yang, Yuan-Ming Li, Yi-Xing Peng, Kun-Yu Lin, Xihan Wei, Jian-Fang Hu, Xiaohua Xie, and Wei-Shi Zheng. Vispeak: Visual instruction feedback in streaming videos. *ICCV*, 2025. 5
- [16] Tianyu Fu, Tengxuan Liu, Qinghao Han, Guohao Dai, Shengen Yan, Huazhong Yang, Xuefei Ning, and Yu Wang. Framefusion: Combining similarity and importance for video token reduction on large visual language models. *ICCV*, 2025. 2
- [17] Google DeepMind. Gemini 2.5 Pro. <https://deepmind.google/models/gemini/pro/>, 2025. 1
- [18] Bo He, Hengduo Li, Young Kyun Jang, Menglin Jia, Xuefei Cao, Ashish Shah, Abhinav Shrivastava, and Ser-Nam Lim. Ma-Imm: Memory-augmented large multimodal model for long-term video understanding. *CVPR*, 2024. 3
- [19] Xiaohu Huang, Hao Zhou, and Kai Han. Prunevid: Visual token pruning for efficient video large language models. In *ACL*, 2025. 3
- [20] Zhenpeng Huang, Xinhao Li, Jiaqi Li, Jing Wang, Xiangyu Zeng, Cheng Liang, Tao Wu, Xi Chen, Liang Li, and Limin Wang. Online video understanding: Ovbench and videochat-online. In *CVPR*, pages 3328–3338, 2025. 2, 6, 8
- [21] Aaron Hurst, Adam Lerer, Adam P Goucher, Adam Perelman, Aditya Ramesh, Aidan Clark, AJ Ostrow, Akila Welihinda, Alan Hayes, Alec Radford, et al. Gpt-4o system card. *arXiv:2410.21276*, 2024. 5
- [22] Peng Jin, Ryuichi Takanobu, Caiwan Zhang, Xiaochun Cao, and Li Yuan. Chat-univi: Unified visual representation empowers large language models with image and video understanding. *CVPR*, 2024. 2
- [23] Lik-Hang Lee and Pan Hui. Interaction methods for smart glasses: A survey. *IEEE access*, 6:28712–28732, 2018. 1
- [24] Jie Lei, Linjie Li, Luowei Zhou, Zhe Gan, Tamara L Berg, Mohit Bansal, and Jingjing Liu. Less is more: Clipbert for video-and-language learning via sparse sampling. In *CVPR*, 2021. 1
- [25] Bo Li, Yuanhan Zhang, Dong Guo, Renrui Zhang, Feng Li, Hao Zhang, Kaichen Zhang, Peiyuan Zhang, Yanwei Li, Ziwei Liu, et al. Llava-onevision: Easy visual task transfer. *arXiv preprint arXiv:2408.03326*, 2024. 1, 2, 5, 6
- [26] Yanwei Li, Chengyao Wang, and Jiaya Jia. Llama-vid: An image is worth 2 tokens in large language models. In *ECCV*, pages 323–340. Springer, 2024. 3

- [27] Junming Lin, Zheng Fang, Chi Chen, Zihao Wan, Fuwen Luo, Peng Li, Yang Liu, and Maosong Sun. Streamingbench: Assessing the gap for mllms to achieve streaming video understanding. *arXiv preprint arXiv:2411.03628*, 2024. 2, 6
- [28] Yang Liu, Weixing Chen, Yongjie Bai, Xiaodan Liang, Guanbin Li, Wen Gao, and Liang Lin. Aligning cyber space with physical world: A comprehensive survey on embodied ai. *IEEE/ASME Transactions on Mechatronics*, 2025. 1, 2
- [29] Muhammad Maaz, Hanoona Rasheed, Salman Khan, and Fahad Shahbaz Khan. Video-chatgpt: Towards detailed video understanding via large vision and language models. In *ACL*, 2024. 2
- [30] Ming Nie, Dan Ding, Chunwei Wang, Yuanfan Guo, Jianhua Han, Hang Xu, and Li Zhang. Slowfocus: Enhancing fine-grained temporal understanding in video llm. *NIPS*, 37: 81808–81835, 2024. 2
- [31] Zhenyu Ning, Guangda Liu, Qihao Jin, Wenchao Ding, Minyi Guo, and Jieru Zhao. Livevlm: Efficient online video understanding via streaming-oriented kv cache and retrieval. *arXiv preprint arXiv:2505.15269*, 2025. 1, 2, 3, 5, 6, 7
- [32] Junbo Niu, Yifei Li, Ziyang Miao, Chunjiang Ge, Yuanhang Zhou, Qihao He, Xiaoyi Dong, Haodong Duan, Shuangrui Ding, Rui Qian, et al. Ovo-bench: How far is your video-llms from real-world online video understanding? In *CVPR*, pages 18902–18913, 2025. 2, 6
- [33] OpenAI. GPT-5. <https://openai.com/gpt-5/>, 2025. 1
- [34] Nobuyuki Otsu. A threshold selection method from gray-level histograms. *IEEE Transactions on Systems, Man, and Cybernetics*, 9(1):62–66, 1979. 2, 3, 4
- [35] Rui Qian, Xiaoyi Dong, Pan Zhang, Yuhang Zang, Shuangrui Ding, Dahua Lin, and Jiaqi Wang. Streaming long video understanding with large language models. *NIPS*, 37: 119336–119360, 2024. 2
- [36] Rui Qian, Shuangrui Ding, Xiaoyi Dong, Pan Zhang, Yuhang Zang, Yuhang Cao, Dahua Lin, and Jiaqi Wang. Dispider: Enabling video llms with active real-time interaction via disentangled perception, decision, and reaction. In *CVPR*, 2025. 5, 6
- [37] Shuhuai Ren, Linli Yao, Shicheng Li, Xu Sun, and Lu Hou. Timechat: A time-sensitive multimodal large language model for long video understanding. In *CVPR*, 2024. 1
- [38] Kele Shao, Keda Tao, Kejia Zhang, Sicheng Feng, Mu Cai, Yuzhang Shang, Haoxuan You, Can Qin, Yang Sui, and Huan Wang. When tokens talk too much: A survey of multimodal long-context token compression across images, videos, and audios. *arXiv preprint arXiv:2507.20198*, 2025. 2
- [39] Xiaoqian Shen, Yunyang Xiong, Changsheng Zhao, Lemeng Wu, Jun Chen, Chenchen Zhu, Zechun Liu, Fanyi Xiao, Balakrishnan Varadarajan, Florian Bordes, et al. Longvu: Spatiotemporal adaptive compression for long video-language understanding. In *ICML*, 2025. 5, 6
- [40] Yan Shu, Peitian Zhang, Zheng Liu, Minghao Qin, Junjie Zhou, Tiejun Huang, and Bo Zhao. Video-xl: Extra-long vision language model for hour-scale video understanding. *CVPR*, 2025. 2, 5
- [41] Enxin Song, Wenhao Chai, Guanhong Wang, Yucheng Zhang, Haoyang Zhou, Feiyang Wu, Haozhe Chi, Xun Guo, Tian Ye, Yanting Zhang, et al. Moviechat: From dense token to sparse memory for long video understanding. In *CVPR*, 2024. 6
- [42] Enxin Song, Wenhao Chai, Tian Ye, Jenq-Neng Hwang, Xi Li, and Gaoang Wang. Moviechat+: Question-aware sparse memory for long video question answering. *PAMI*, 2025. 2, 3
- [43] Xi Tang, Jihao Qiu, Lingxi Xie, Yunjie Tian, Jianbin Jiao, and Qixiang Ye. Adaptive keyframe sampling for long video understanding. *CVPR*, 2025. 5
- [44] Yunlong Tang, Jing Bi, Siting Xu, Luchuan Song, Susan Liang, Teng Wang, Daoan Zhang, Jie An, Jingyang Lin, Rongyi Zhu, et al. Video understanding with large language models: A survey. *IEEE Transactions on Circuits and Systems for Video Technology*, 2025. 2
- [45] Keda Tao, Can Qin, Haoxuan You, Yang Sui, and Huan Wang. Dycoke: Dynamic compression of tokens for fast video large language models. In *CVPR*, 2025. 3
- [46] Gemini Team, Petko Georgiev, Ving Ian Lei, Ryan Burnell, Libin Bai, Anmol Gulati, Garrett Tanzer, Damien Vincent, Zhufeng Pan, Shibo Wang, et al. Gemini 1.5: Unlocking multimodal understanding across millions of tokens of context. *arXiv:2403.05530*, 2024. 5
- [47] Haibo Wang, Bo Feng, Zhengfeng Lai, Mingze Xu, Shiyu Li, Weifeng Ge, Afshin Dehghan, Meng Cao, and Ping Huang. Streambridge: Turning your offline video large language model into a proactive streaming assistant. *NIPS*, 2025. 1, 2, 4
- [48] Junke Wang, Dongdong Chen, Zuxuan Wu, Chong Luo, Luwei Zhou, Yucheng Zhao, Yujia Xie, Ce Liu, Yu-Gang Jiang, and Lu Yuan. Omnivl: One foundation model for image-language and video-language tasks. In *NeurIPS*, 2022. 1
- [49] Junke Wang, Xitong Yang, Hengduo Li, Li Liu, Zuxuan Wu, and Yu-Gang Jiang. Efficient video transformers with spatial-temporal token selection. In *ECCV*, 2022. 2
- [50] Junke Wang, Dongdong Chen, Chong Luo, Xiyang Dai, Lu Yuan, Zuxuan Wu, and Yu-Gang Jiang. Chatvideo: A tracklet-centric multimodal and versatile video understanding system. *arXiv preprint arXiv:2304.14407*, 2023. 1
- [51] Junke Wang, Lingchen Meng, Zejia Weng, Bo He, Zuxuan Wu, and Yu-Gang Jiang. To see is to believe: Prompting gpt-4v for better visual instruction tuning. *arXiv preprint arXiv:2311.07574*, 2023. 2
- [52] Junke Wang, Dongdong Chen, Chong Luo, Bo He, Lu Yuan, Zuxuan Wu, and Yu-Gang Jiang. Omnivid: A generative framework for universal video understanding. In *CVPR*, 2024. 2
- [53] Weiyun Wang, Zhangwei Gao, Lixin Gu, Hengjun Pu, Long Cui, Xingguang Wei, Zhaoyang Liu, Linglin Jing, Shenglong Ye, Jie Shao, Zhaokai Wang, Zhe Chen, Hongjie Zhang, Ganlin Yang, Haomin Wang, Qi Wei, Jinhui Yin, Wenhao Li, Erfei Cui, Guanzhou Chen, Zichen Ding, Changyao Tian, Zhenyu Wu, Jingjing Xie, Zehao Li, Bowen Yang, Yuchen Duan, Xuehui Wang, Zhi Hou, Haoran Hao, Tianyi Zhang, Songze Li, Xiangyu Zhao, Haodong Duan, Nianchen Deng, Bin Fu, Yinan He, Yi Wang, Conghui He, Botian Shi, Junjun He, Yingting Xiong, Han Lv, Lijun Wu, Wenqi Shao,

- Kaipeng Zhang, Huipeng Deng, Biqing Qi, Jiaye Ge, Qipeng Guo, Wenwei Zhang, Songyang Zhang, Maosong Cao, Junyao Lin, Kexian Tang, Jianfei Gao, Haiyan Huang, Yuzhe Gu, Chengqi Lyu, Huanze Tang, Rui Wang, Haijun Lv, Wanli Ouyang, Limin Wang, Min Dou, Xizhou Zhu, Tong Lu, Dahua Lin, Jifeng Dai, Weijie Su, Bowen Zhou, Kai Chen, Yu Qiao, Wenhai Wang, and Gen Luo. Internvl3.5: Advancing open-source multimodal models in versatility, reasoning, and efficiency. *arXiv preprint arXiv:2508.18265*, 2025. 1
- [54] Yueqian Wang, Xiaojun Meng, Yuxuan Wang, Jianxin Liang, Jiansheng Wei, Huishuai Zhang, and Dongyan Zhao. Videollm knows when to speak: Enhancing time-sensitive video comprehension with video-text duet interaction format, 2024. 4
- [55] Yi Wang, Xinhao Li, Ziang Yan, Yinan He, Jiashuo Yu, Xiangyu Zeng, Chenting Wang, Changlian Ma, Haiyan Huang, Jianfei Gao, Min Dou, Kai Chen, Wenhai Wang, Yu Qiao, Yali Wang, and Limin Wang. Internvideo2.5: Empowering video mllms with long and rich context modeling. *arXiv preprint arXiv:2501.12386*, 2025. 2
- [56] Yuetian Weng, Mingfei Han, Haoyu He, Xiaojun Chang, and Bohan Zhuang. Longvlm: Efficient long video understanding via large language models. In *ECCV*, pages 453–470. Springer, 2024. 3
- [57] Haoning Wu, Dongxu Li, Bei Chen, and Junnan Li. Longvideobench: A benchmark for long-context interleaved video-language understanding. *NeurIPS*, 2024. 2, 6
- [58] Haomiao Xiong, Zongxin Yang, Jiazuo Yu, Yunzhi Zhuge, Lu Zhang, Jiawen Zhu, and Huchuan Lu. Streaming video understanding and multi-round interaction with memory-enhanced knowledge. In *ICLR*, 2025. 1, 2, 6
- [59] Ruyi Xu, Guangxuan Xiao, Yukang Chen, Liuning He, Kelly Peng, Yao Lu, and Song Han. Streamingvlm: Real-time understanding for infinite video streams. *arXiv preprint arXiv:2510.09608*, 2025. 1, 2
- [60] Senqiao Yang, Yukang Chen, Zhuotao Tian, Chengyao Wang, Jingyao Li, Bei Yu, and Jiaya Jia. Visionzip: Longer is better but not necessary in vision language models. In *CVPR*, 2025. 3
- [61] Yanlai Yang, Zhuokai Zhao, Satya Narayan Shukla, Aashu Singh, Shlok Kumar Mishra, Lizhu Zhang, and Mengye Ren. Streammem: Query-agnostic kv cache memory for streaming video understanding. *arXiv preprint arXiv:2508.15717*, 2025. 1, 2, 3, 6
- [62] Linli Yao, Yicheng Li, Yuancheng Wei, Lei Li, Shuhuai Ren, Yuanxin Liu, Kun Ouyang, Lean Wang, Shicheng Li, Sida Li, et al. Timechat-online: 80% visual tokens are naturally redundant in streaming videos. In *ACM MM*, 2025. 1, 2, 4, 5, 6, 7, 8
- [63] Xiangyu Zeng, Kefan Qiu, Qingyu Zhang, Xinhao Li, Jing Wang, Jiabin Li, Ziang Yan, Kun Tian, Meng Tian, Xinhai Zhao, et al. Streamforest: Efficient online video understanding with persistent event memory. *NIPS*, 2025. 1, 5, 6
- [64] Hang Zhang, Xin Li, and Lidong Bing. Video-llama: An instruction-tuned audio-visual language model for video understanding. *EMNLP*, 2023. 2
- [65] Haoji Zhang, Yiqin Wang, Yansong Tang, Yong Liu, Jiashi Feng, Jifeng Dai, and Xiaojie Jin. Flash-vstream: Memory-based real-time understanding for long video streams. In *ICCV*, 2025. 1, 2, 5, 6
- [66] Peiyuan Zhang, Kaichen Zhang, Bo Li, Guangtao Zeng, Jingkang Yang, Yuanhan Zhang, Ziyue Wang, Haoran Tan, Chunyuan Li, and Ziwei Liu. Long context transfer from language to vision. *arXiv preprint arXiv:2406.16852*, 2024. 5, 6
- [67] Yuanhan Zhang, Jinming Wu, Wei Li, Bo Li, Zejun Ma, Ziwei Liu, and Chunyuan Li. Llava-video: Video instruction tuning with synthetic data. *arXiv preprint arXiv:2410.02713*, 2024. 2, 5, 6
- [68] Junjie Zhou, Yan Shu, Bo Zhao, Boya Wu, Zhengyang Liang, Shitao Xiao, Minghao Qin, Xi Yang, Yongping Xiong, Bo Zhang, Tiejun Huang, and Zheng Liu. Mlvu: Benchmarking multi-task long video understanding. In *CVPR*, 2025. 2, 6, 8